Discovery of a conserved rule behind the assembly of β-barrel membrane proteins

Edward M. Germany[1], Nakajohn Thewasano[1], Kenichiro Imai[2], Yuki Maruno[1], Rebecca S. Bamert[3,4], Rhys A. Dunstan[3,4], Yue Ding[5,6], Yukari Nakajima[1], XiangFeng Lai[5], Chaille T. Webb[3,4], Christopher J. Stubenrauch[3,4], Kentaro Hidaka[1], Kher Shing Tan[3,4], Hsin-Hui Shen[5,6,*], Trevor Lithgow[3,4,*], and Takuya Shiota[1,*]

[1]Organization for Promotion of Tenure Track, University of Miyazaki, Nishi 1-1 Gakuen Kibanadai, Miyazaki, 889-2192, Japan

[2]Cellular and Molecular Biotechnology Research Institute, National Institute of Advanced Industrial Science and Technology (AIST), 2-4-7 Aomi, Koto-ku, Tokyo 135-0064, Japan

[3]Centre to Impact AMR, Monash University, Clayton, VIC 3800, Australia

[4] Infection & Immunity Program, Biomedicine Discovery Institute, and Department of Microbiology, Monash University, Clayton, VIC 3800, Australia

[5]Department of Materials Science and Engineering, Monash University, Clayton, VIC 3800, Australia

[6]Biomedicine Discovery Institute and Department of Biochemistry and Molecular Biology, Monash University, Clayton 3800, Australia

[*]e-mail: takuya_shiota@med.miyazaki-u.ac.jp (T.S.), hsin-hui.shen@monash.edu (H.H.S.), trevor.lithgow@monash.edu (T.L.)

ABSTRACT

Gram-negative bacteria, mitochondria and chloroplasts contain β-barrel outer membrane proteins (OMPs). The current dogma holds that most OMPs have a "β-signal" imprinted in the final β-strand and assembly machineries capture it for the folding and membrane insertion of the OMP. Here, we reveal an additional rule that a sequence equivalent to the β-signal is repeated in a second β-strand of the same orientation as the final β-signal, within both bacterial and mitochondrial OMPs. The internal signal promotes efficiency in the assembly reaction of these OMPs. In Gram-negative bacteria BamD, an essential subunit of the bacterial β-barrel assembly machinery (BAM), can recognize both signals, marshalling several β-strands for rapid OMP for assembly. The internal signal-BamD marshalling system is not essential for bacterial viability, but is necessary to retain the integrity of the outer membrane to against antibiotics and other environmental insults.

Main

In Gram-negative bacteria and mitochondria, the organelles derived from them, outer membrane proteins (OMPs) play important roles in membrane-mediated processes[1]. The major OMPs are composed of β-barrel transmembrane domains. Each OMP β-barrel spans the membrane as a cylindrical structure formed from amphiphilic, antiparallel β-strands, stabilized in the tertiary barrel structure by hydrogen bonds between the first and last β-strands (the β-seam)[2,3] . The fundamental chaperones for OMP assembly are the members of the Omp85 protein superfamily, conserved across bacterial lineages and organelles[4–7]. The Omp85 superfamily are themselves β-barrel proteins, and the β-seam in their own structure - the lateral gate - is the catalytic site of the OMPs assembly. Structural and biochemical approaches have revealed that the first strand of the lateral gate interacts with the last strand of client OMPs (substrates)[8–14]. Most of the substrate contains conserved motif termed "β-signal" at the last strand[15–18].

The Omp85 protein BamA is a ubiquitous chaperone for β-barrel assembly in bacteria[19]. In *E. coli*, BamA associates with a set of four lipoproteins to form a hetero-oligomeric chaperone called the β-barrel Assembly Machinery (BAM) complex[20–22]. While the subunit composition of the BAM complex varies in different bacterial lineages, it is an essential feature of all bacteria with an outer membrane[23,24]. Of the four lipoprotein subunits in *E. coli*: BamB-E[16–18], only BamA and BamD are essential for viability, and each of these subunits are found in all bacterial lineages[19,24,25].

While embedded in the outer membrane, BamA projects an extensive N-terminal domain into the periplasm, consisting of five polypeptide transport-associated (POTRA) domains[8,26]. BamD is docked to the POTRA domains, contributing to a large, funnel-like periplasmic feature of the BAM complex in the periplasm[16–18,23]. Recent focus on the interaction between the lateral gate of BamA and the β-signal in substrate has been made possible through obtaining snap-shot structures of assembly intermediates bound to the lateral gate[9,12,27] as well as the isolation of inhibitory compounds such as darobactin capable of entering the lateral gate of BamA to exert a lethal effect on *E. coli*[10,28,29].

Despite these recent advances, the molecular mechanism of OMP assembly is enigmatic. In terms of the β-signal which has been shown to be important for targeting

and folding of substrate[15,16], several important OMPs do not have a recognizable β-signal motif in their C-terminal β-strand. BamA is one such OMP[30] and, in a comprehensive study of another class of OMPs called autotransporters, hidden Markov model analysis showed that while 1038 non-redundant proteins had a C-terminal β-motif, there were 473 non-redundant proteins that had a β-motif only in internal strands[31]. Are these internal motifs functioning as β-signals? How could that work given that the current dogma dictates that a β-signal should engage the first strand of the lateral gate in BamA[32,33]. Furthermore, BamD has been suggested to bind the C-terminal β-signal[30], but it remains unclear how this binding could be mediated and uncertain what role this interaction could play in OMP assembly.

Here, we established a screening system based on an *in vitro* reconstituted membrane assay using the *E. coli* Microsomal Membrane (EMM)[34] and revealed that most of OMPs, including the major porins that are the predominant substrate of the BAM complex, contain two β-signal related repeats: the C-terminal β-signal and an equivalent internal repeat of this sequence motif, which occurs in the same orientation as the final strand. A comparison of the internal and C-terminal β-signals revealed the essential elements of the signal that are recognized by the BAM complex. Internal β-signals are recognized by BamD and are responsible for rapid assembly of the OMP into the bacterial membrane. Comparative genome sequence analysis revealed these internal β-signals are also conserved in mitochondrial OMPs. Moreover, in Gram-negative bacteria, *in situ* cross-linking studies and mutagenesis demonstrated how BamD simultaneously recognized the multiple β-signals, in the context of a functional BAM complex.

.

Results

Identification of essential signal element of bacterial β-signal by the peptidomimetics derived from *E. coli* OmpC.

The EMM assembly assay provides a means for *in vitro* reconstitution of BAM complex function, where the assembly of a radio-labelled OMP, in this case ^{35}S-labelled OmpC, can be monitored over time (Extended Data Fig. 1a)[34]. To screen for potential peptidomimetics that could inhibit BAM complex function, a synthetic peptide library was designed for coverage of the sequence features in OmpC (Extended Data Fig. 2a). As a second unrelated OMP, we also assayed the autotransporter EspP to assess competitive inhibition efficiency. Autotransporters have two domains; (1) a β-barrel domain, assembled into the OM by the BAM complex, and (2) a passenger domain, which traverses the OM via the lumen of the β-barrel domain itself and is subsequently cleaved by the correctly assembled β-barrel domain[35]. Once the barrel domain is assembled into the membrane it becomes protease-resistant, with residual unassembled and passenger domains degraded[36,37]. Under the conditions of the EMM assay, EspP was observed to fragment as predicted (Fig. 1a and Extended Data Fig. 1b) and was used to rapidly screen inhibitory peptides in a robust high-throughput format.

Six peptides (4, 10, 17, 18, 21, and 23) were found to inhibit EspP maturation (Fig. 1b). All of the inhibitor peptides except peptide 10 which was less than 20% inhibition efficiency, inhibited the other four model substrates, porins OmpC and OmpF, the OM-peptidoglycan bridge OmpA, and the maltoporin LamB (Fig. 1 c, d, e and Extended Data Fig. 2b, c), implying that these peptides inhibited a common assembly system, the BAM complex. Hagan and co-workers used the peptides derived from C-terminal regions of BamA to inhibit the BAM function *in vitro* and showed that the third to the C-terminal strand (-3 strand) had inhibition ability, but not the last strand (-1 strand)[30]. We unbiasedly collected all of peptides containing the [Ω/Φ]x[Ω/Φ] motif which is commonly conserved motif in the β-signal (ζxGxx[Ω/Φ]x[Ω/Φ], where ζ, is any polar residue; G is a glycine residue; Ω is any aromatic residue; Φ is any hydrophobic residue and x is any residue)[15,30]. and compared the sequences difference between inhibitor peptides and non-inhibitor (Fig. 1f). The inhibitor peptides commonly contained a hydrophobic or aromatic residue upstream of one of the polar residues, but not the polar and Gly residues. Interestingly, peptide 9, which contains elements of the β-signal, did not show inhibition of EpsP. EMM assembly assay using amino-acid

substituted peptide derived from peptide 18 revealed that the Ω or Φ at position 0 (0Φ) in addition to the [Ω/Φ]x[Ω/Φ] motif is necessary to be recognized by the BAM complex (Fig. 1g). Peptide 24 is derived from yeast-Tom40, a β-barrel protein from mitochondria[38], which does not have this hydrophobic residue, meaning that the essential elements of the bacterial β-signal are Φxxxxx[Ω/Φ]x[Ω/Φ].

Mutations in the β-strands of OmpC impact on assembly.

In order to validate if these peptides mimicked β-signal or had a real affinity region to the BAM complex, we analyzed peptide regions, sequence conservation, and assembly efficiency of each mutant of OmpC. Due to the lack of sequence conservation in peptide 4 we did not expect this to be a universal motif required for assembly, and this was confirmed by the inability of any of the single mutants to retain any inhibitory activity (Fig 2a). Since peptide 17 and peptide 18 overlap, they were considered together. This means that, when considered as a single region, all peptide regions except peptide 4 included the first (-1), third (-3), and fifth (-5) beta strands from the C-terminal side. Given the antiparallel structure of a β-barrel, the three strands have the same orientation, and conform to the motif Φxxxxx[Ω/Φ]x[Ω/Φ]. One minor difference is that in the -1 strand, the motifs are all contained within the β strand, whereas in the -5 strand, the C-terminaous of the motifs were present in the post-strand loop. The structurally corresponding [Ω/Φ]x[Ω/Φ] motif in peptide 23 of peptide 21 was not the predicted YKI339 but the more N-terminal YYF327 (Fig. 2a). Among the mutants with significantly reduced assembly efficiency, as estimated from trimer formation efficiency on BN-PAGE, Y286A, Y325A, and Y365A correspond to Ω/Φ in position 6 (Ω/Φ), and F280A corresponds to 0Φ of the putative signal (Fig. 2a and Extended Data Fig. 6a).

Although the -3 strand's β-signal has been reported important for BamA assembly previously[30], it was intriguing to discover an important assembly determinant in the -3 or -5 strand, as it is substantially distant from the C-terminal region that engages with the BAM complex to initiate what is considered to be a passive strand-by-strand assembly reaction[33]. Thus, we analyzed the -3 and -5 strands in more detail, focusing on conserved residues present in both strands. Sequence conservation analysis suggested conservation in the equivalent b-strands of OMPs whose structures have been determined (Extended Data Fig. 3, 4, and 5). To distinguish β-signals in the

-3 or -5 strand from the canonical C-terminal β-signal, they are called the "internal β-signal", and we analyzed the -5 strand internal β-signal, which locates more internal, more as a representative internal β-signal. We constructed mutants in 0Φ or 6[Ω/Φ] of the -5 strand in OmpF and LamB, respectively (Fig. 2b). BN-PAGE analysis showed these residues were important for the assembly of OmpF and LamB (Fig. 2c and Extended Data Fig. 6b).

To determine whether the internal β-signal was necessary for assembly in vivo, we constructed the arabinose inducible plasmid expressing mutants of 0Φ, 6[Ω/Φ] or both positions in either -5 or -1 strands of OmpC. To distinct plasmid OmpC variants from endogeneous OmpC, we introduced a FLAG epitope tag into the N-terminal region of OmpC, immediately behind the cleavage site for the SEC-signal sequence (Fig. 2d)[39]. Expression of FLAG-OmpC variants induced by 0.1% arabinose was confirmed through immunoblotting of total cell lysate (Fig. 2e) In the respective EMM fractions, the protein levels of FLAG-OmpC variants were equivalent, but with a marked reduction seen in the steady-state level of the double (“FY” or "VY") mutants OmpC(F280A, Y286A or V359A, Y365A) (Fig. 2f). On BN-PAGE analysis, the FLAG-OmpC runs as two forms, with the upper form corresponding in size to the native trimer (Fig. 2g top). Dimeric forms of OmpC have been seen previously and shown to have structural and functional properties equivalent to trimers[40]. Both double mutants displayed drastic reductions of the dimer and trimer. As a control, the level and integrity of the BAM complex were monitored and found to be equivalent in all conditions (Fig. 2f, and g bottom). Taken together these results suggest that internal β-signal was also important for assembly as canonical β-signal.

The internal signal is responsible for insertion into OM.

We sought to reveal the role of internal β-signal for assembly. Analysis via BN-PAGE showed the formation of a high-molecular-weight product during assay of the internal β-signal mutant (Y286A) forms of these OMPs (Fig. 3a). A “gel shift” BN-PAGE analysis was used to directly determine if the high molecular weight form of ^{35}S-labelled Y286A was in contact with the BAM complex. The addition of an antibody recognizing the surface-exposed component BamC to detergent-solubilized EMM fraction prior to electrophoresis, resulted in a dramatic shift (i.e. retardation due to the

added mass of antibodies) of the intermediate ("Int"), consistent with OmpC-Y286A being a stable assembly intermediate engaged with the BAM complex (Fig. 3b). To determine when this assembly intermediate formed, we performed urea extraction after EMM assembly assay and analyzed the urea-resistant pellet by BN-PAGE. The trimer form of OmpC was not extracted by urea, indicating that correctly assembled OmpC is fully inserted into OM (Fig. 3c). The intermediate was completely extracted with urea, as expected for a substrate engaged in protein-protein interactions with the EMM fraction (i.e. the BAM complex). These results suggest that the mutant OmpC interacts with the BAM complex, but is not yet inserted into the membrane environment of the EMM.

Despite the myriad structures depicting BAM complex binding of substrates in the membrane embedded barrel domain, there is a dearth of information regarding binding of substrates to the periplasmic BAM components. Neutron reflectometry (NR) is a powerful tool for probing these types of substrate-chaperone interactions, and assessing the dynamics of substrate-binding, ideally suited for membrane-embedded proteins[41]. To apply NR imaging to understand the engagement of OmpC with the BAM complex, BamA was immobilized on an Ni-NTA atomic flat gold-coated silicon wafer to orient the POTRA domain distal to the silicon wafer as previously described[42]. A lipid layer was reconstituted to provide BamA with a membrane-like environment (Fig. 3d). To evaluate these additions, the following were sequentially measured by NR: (i) BamA with lipid (1st measurement), (ii) BamA with lipid and BamD (2nd measurement), and (iii) BamA-BamD-lipid with the addition of OmpC(WT) or OmpC(Y286A) (3rd measurement) (Extended Data Fig. 7a). Comparing the reflectivity profiles of three measurements (Fig. 3d), the addition of BamD and OmpC(Y286A), changes were observed in the layers after the addition of BamD and OmpC(Y286A), as seen in a shift of fringe to low Q range around 0.02-0.03 Å-1.

Based on crystal structures, the periplasmic domains of BamA can be treated as two rigid bodies: POTRA1-2(P1-2) and POTRA3-5(P3-5). Thus, for further data analysis, we divided BamA into four layers: the His6 extra-cellular layer where BamA is attached to the chip, the membrane layer (containing the β-barrel domain of BamA), an adjoining POTRA3-5 layer and the N-terminal POTRA1-2 layer. Analysis of the data showed any variation in thickness of these layers, which corresponds to the position of the additional subunit, at each point of measurement (Fig. 3e, Extended Data Fig. 7b, c). At the 2nd

measurement, the SLD profiles showed that BamD was located in the P3-5 layer (Figure 3e, Extended Data Fig.7d, e), an observation consistent with previous studies on the resting BAM complex[43]. The 3rd measurement, only the addition of the OmpC(Y286A) substrate revealed binding, and this binding was to the P3-5 layer, with an extension of this layer from 29.7±0.8 Å to 45.5±1.6 Å away from the membrane (Fig. 3e, f, Extended Data Fig. 7f, g). The P3-5 roughness was lower than the β-barrel domain and P1-2, but the Y286A-binding reversed their roughness of them, implying that the P3-5 region can flexibly accept the substrate. By contrast, no clear reflection changes were observed on the addition of OmpC(WT), implying that interaction of the unmodified substrate with the BAM complex on the Si-Wafer was resolved too quickly to capture any binding intermediates (Extended Data Fig. 8). The failure to observe changes with the WT-OmpC control in the NR analysis is consistent with the data from the EMM assembly assay, where we show that WT-OmpC does not form a stable intermediate across a 60-minute time course (Fig. 3a). These findings indicate that OmpC(Y286A) is stacked at a position with the POTRA3-5 and BamD layer, and that the Y286A mutation results in a relatively static binding to this specific periplasmic region of the BAM complex.

The aromatic residue of the canonical β-signal is important for recognition by the BAM complex, but is also important for spontaneous folding of purified OMPs in the absence of the BAM complex[44]. To test whether the internal β-signal is also important for spontaneous folding, we purified the urea-denatured OmpC(Y286A) and the canonical β-signal mutant OmpC(Y365A) to compare the rate of folding relative to OmpC(WT). The spontaneous folding of each OmpC variant was assessed by the rate of formation of trimer in detergent micelles (Fig. 3g). Trimer embedded into detergent micelles migrated at 100 kDa in this assay system, whereas non-folded monomeric OmpC migrated at 37 kDa. Relative to the rate/extent of trimer formation observed for OmpC(WT), both signal mutants showed significantly impaired spontaneous folding.

BamD interacts with both canonical and internal β-signals with distinct regions.

We sought to determine the receptor for the internal β-signal. In vitro binding assays showed that both BamA and BamD can independently bind to the OmpC polypeptide (Extended Data Fig. 9). We therefore pre-incubated either BamA or BamD with signal containing inhibitor peptides, 18, 21, or 23, to interfere with OmpC binding

(Fig. 4a). Peptide 23 inhibited binding of the substrate by BamA, whereas peptide 18 inhibited binding of the substrate by BamD. Peptide 21 inhibited binding of the substrate by both BamA and BamD. This suggests the internal β-signal preferentially interacts with BamD.

We then sought to elucidate the residues within BamD that mediate this signal-receptor interaction. As a first screening, we applied *in vitro* site-specific photo-crosslinking to determine the substrate-binding region of BamD (Extended Fig.10a). A library of 40 BamD variants was created to incorporate the non-natural amino acid, *p*-benzoyl-$_L$-phenylalanine (BPA), by the suppressor tRNA method in a series of positions[45]. The UV-dependent appearance of crosslinks between OmpC and BamD occurred for 17 of the BamD variants (Extended Data Fig. 10b, c). The analysis was repeated to determine BamD cross-links for ^{35}S-labelled OmpC(WT), the -5 signal mutant OmpC(Y286A), or the β-signal mutant OmpC(βAAA: Y365A, Q366A, F367A) (Extended Data Fig. 10d, e). This mapping of OmpC binding showed that an N-terminal section of BamD (amino acid residues 60 or 65) interacts with the internal β-signal, while a C-terminal section of BamD (amino acid residues 196, 200, 204) interacts with canonical β-signal (Extended Data Fig. 10f). BPA crosslinking provide the

While *in vitro* site-specific photo-crosslinking provides information on the substrate receptor region of BamD, only indirectly does it measure which residues of OmpC are being recognized. In order to obtain complimentary data on OmpC binding by BamD, we purified a form of BamD that is substituted with a cysteine residue in the substrate-binding region, and synthesized forms of ^{35}S-labeled OmpC substituted with a cysteine residue at various positions. Treatment with 1 μM $CuSO_4$ can stimulate disulfide formation between BamD and OmpC (Fig. 4b). Consistent with the BPA crosslinking data, the positions near the -5 signal in OmpC (amino acid residues 278, 284, 296 and 302) formed disulfide bonds with the N-terminal section of BamD (amino acid residues 49, 60). Conversely, residues towards the C-terminal, canonical β-signal of OmpC (amino acid residues 333, 357, and 363) formed disulfide bonds with a C-terminal section of BamD (at amino acid residue 204) (Fig 4c). All of disulfide crosslinked products were validated by reducing condition SDS-PAGE (Extended Data Fig. 11).

To further confirm this interaction, we expressed BPA-containing BamD and FLAG-tagged OmpC (substrates) and performed *in vivo* photocrosslinking (Fig. 4d).

BamD with BPA at positions 49, 53, 65, or 196 were crosslinked to FLAG-OmpC, but not 114 and 200. All of the crosslinked positions corresponded to *in vitro* BPA and disulfide crosslinking studies. All positions except 114 are facing the interior of the funnel-like structure of the periplasmic domain of the BAM complex, changed crosslinking intensity by substrate expression, suggesting that the interior of the funnel changes interaction in response to substrate binding. Position 114 locates outside of the funnel and close to BamC on the structure, implying that the outside region stably interacts with other subunits to keep the architecture of the funnel.

Impact of the BamD interaction with both canonical and internal β-signals on OMPs assembly.

To determine if BamD stimulated the assembly of the C-terminus of OMPs, we substituted cysteine residues for amino acids that were outward-facing on the folded OmpC and close to each other on the adjacent β-strand (Fig. 5a). Samples harboring cysteine residues in OmpC that were incubated with BamD migrated faster than non-Cys OmpC on non-reducing SDS-PAGE (Fig. 5b). This migration difference was not observed in reducing conditions, indicating the faster migration occurred as a result of internal molecule disulfide bond formation. Disulfide bonds were formed in all of the paired strands in the final five β-strands. These results suggest that BamD stimulates partial folding of C-terminal five strands of BamD.

We then validated the role of BamD in more physiological conditions. Using substrate binding sites of BamD as landmarks, mapping of sequence conservation across the surface of BamD revealed conserved residues in both the N- and C-terminus, overlapping with residues identified via crosslinking (Fig. 5c). We constructed the mutant of highly conserved amino acids, an internal β-signal binding site mutant (Y62A) and a canonical β-signal mutant (R197A) of BamD, respectively. A bamD depletion strain with endogenous bamD expression controlled by an arabinose-responsive promoter was transformed with a plasmid encoding either of these mutant proteins (Fig. 5d and Extended Data Fig. 12). Growth conditions were established wherein we could deplete endogenous BamD and still not disturb cell growth (Extended Data Fig. 13a). Isolated EMM from the determined time point showed that neither the BamD(Y62A) nor the BamD(R197A) mutants affected the

steady-state protein levels of other components of the BAM complex (Extended Data Fig. 13b), and nor the assembly of the BAM complex (Fig. 5e, Extended Data Fig. 13c). The EMM assembly assay showed that the -5 signal binding site was as important as the β-signal binding site to the overall assembly rates observed for OmpC (Fig. 5f), OmpF (Extended Data Fig. 13d), and LamB (Extended Data Fig. 13e). These results suggest that recognition of both canonical β-signal and internal β-signal by BamD is important for efficient protein assembly.

BamD is responsible for rapid assembly to retain outer membrane integrity.

While BamD function is essential for cell viability (see bamD depletion strain "vector"; Fig. 6a), both individual mutations and double mutation in the ligand-binding site of BamD were not (Extended Data Fig. 13a). This suggests that each mutant compromises a partial function of BamD. To test this hypothesis, we isolated EMM from each mutant strain cultured prolonged, and checked the steady-state level of porins and the BAM complex subunits in each strain (Fig. 6b). The level of the porins OmpA and OmpC/OmpF was less in both the BamD(Y62A) and BamD(R197A) mutants, relative to the level of each component of the BAM complex. This was also true when the level of trimeric OmpF was assessed by native PAGE: less OmpF trimer had been assembled over the growth period relative to the steady-state level of the BAM complex (Fig. 6c).

Vancomycin sensitivity is a classic assay to measure membrane integrity in Gram-negative bacteria. The drug vancomycin cannot permeate the outer membrane of *E. coli* but, if membrane integrity is assaulted by any means then sensitivity to vancomycin is seen[46]. BamD(Y62A) showed impaired OM integrity, while BamD(R197A) was less susceptible to vancomycin treatment (Fig. 6d, e). Similarly, the FY mutant of the OmpC expressing cell was also sensitive to vancomycin, but not the VY mutant (Fig. 6f, g). Interestingly, FY expressing cells decreases the correctly assembled endogeneous OmpF, but not VY (Fig. 6i). This data shows that the N-terminal TPR region of BamD contributes a crucial function to the role of BamD in the BAM complex.

Repeating β-signal rules are conserved in mitochondrial OMPs.

Having established that the internal β-signal is crucial for assembly of OMPs in bacteria, we asked if a similar conserved feature was present in mitochondrial OMPs. While the mitochondrial and bacterial assembly systems have evolved significant differences, there are also distant evolutionary echoes that unite them[47]. Analysing the 3D structure and sequence of mitochondrial OMPs revealed that there are internal β-signal sequences the polar residue, the Gly residue, and [Ω/Φ]x[Ω/Φ] sequence signature are all well conserved (Fig. 7a, b and Extended Data Fig. 14). However, testing whether the internal β-signal in mitochondrial OMPs is important for assembly requires a functional assay, so we constructed a series of mutations designed to impact on the putative internal β-signal of the mitochondrial protein Tom40. A well-characterized assay to measure the assembly of Tom40 exists and can be interrogated as follows: (i) newly synthesized Tom40is translocated into mitochondria, (ii) in the intermembrane space Tom40 is bound to the SAM (sorting and assembly machinery) complex – the mitochondrial equivalent of the BAM complex, (iii) an assembly intermediate of Tom40 is arrested by the SAM complex until other subunits arrive, with this arrested form observed on BN-PAGE as a 250 kDa complex (Int. I in Fig. 7c). (iv) as subunits of the TOM complex arrive to stimulate release from the SAM complex, a Tom40 intermediate II is observed as a 100 kDa complex (Int. II in Fig. 7c), and (v) Finally Tom40 forms the TOM core complex (TOM in Fig. 7c)[15].

When ^{35}S-labelled Tom40 was incubated with mitochondria, the internal signal mutants (Y307A or Y309A) slightly impaired the formation of int. I, and the triple internal signal mutants (Y307A, E308A, Y309A) completely impaired the formation of Int. I. Chase experiments showed that once formed assembly Int. I, an internal β-signal mutant correctly formed the TOM complex via the Int. II, indicating that the internal β-signal is only responsible for the conserved assembly process, which is insertion into OM (Fig. 7d). Taken together, the rule, repeating the signal at the same orientation strands of the C-terminal side (-5 or -3 strand), was conserved in mitochondrial OMPs.

Discussion

Previous studies using hidden Markov model analysis showed that in the sub-class of OMPs called autotransporters, 1038 non-redundant proteins contain a C-terminal β-signal motif and, in all of those cases, a second occurrence of the β-signal motif occurred at the -5 strand[48]. The same study showed that 473 non-redundant proteins had no β-signal motif at the C-terminal strand, but rather at the -5 strand and a second β-signal motif in a more N-terminal strand[31]. In our current study, peptidomimetic screening assays focused on major porins provided experimental evidence that internal β-signals are important for assembly into OM.

When conserved sequence features are found via hidden Markov model approaches like HMMR[49] and a sequence motif is defined by tools such as MEME[50], there is information from across many (sometimes hundreds of) non-redundant protein sequences. This rich information can be oversimplified when written as a primary structure description, such as ζxGxx[Ω/Φ]x[Ω/Φ], which is the description typically used for the β-signal[15]. This format for the motif suggests a very equivocal sequence constraint, whereas the reverse may be true: there is a strong tendency for specific residues in each position if the β-motif is to function as a β-signal. However, our peptidomimetics proposed that Φxxxxx[Ω/Φ]x[Ω/Φ] motif bind the BAM complex efficiently (Fig. 1).

It had naturally been assumed that the information contained in the β-signal was important for the initial engagement into the lateral gate of BamA[9,10,12,13,30,51–54]. This no longer needs to be the case due to observations concerning the absence of a β-signal motif in the sequence of the C-terminal strand of some OMPs. We suggest that the information content encoded in the β-signal is to ensure engagement and binding with the BAM complex, but that engagement of the C-terminal strand in the BamA lateral gate may need nothing more than the fact that it is the C-terminal most part of the substrate that is able to form a β-strand antiparallel to the first strand of the BamA β-barrel domain. Our *in vitro* protein folding assay of OmpC demonstrated that the internal β-signal contributes to the spontaneous OMP folding in a similar fashion to the canonical β-signal, which was reported previously. (Fig. 3g)[44]. Thus, the β-signal motif is a sophisticated sequence that combines a signal recognized by a receptor, as well as important elements for folding and stabilization. Having multiple sophisticated sequences may advance efficient assembly. While in mitochondria a BamD-equivalent

is not conserved and the POTRA domain is non-essential for the SAM complex, multiple β-signal motifs remain conserved and necessary for mitochondrial OMPs assembly (Fig. 7). This indicates mitochondria utilize insertion via the lateral gate and assembly acceleration by multiple β-signal.

Our pull-down assay identified the BamD as the primary receptor of the internal β-signal (especially the -5 strand). The introduction of BPA at position F1214, the aromatic residue in what we refer to here as the internal β-signal, cross-linked with BamD during the course of EspP assembly[35]. The crosslinking studies in this work showed that BamD can recognize two distinct features of a substrate: the internal β-signal, and the canonical C-terminal β-signal, by the N-terminal region and C-terminal region, respectively (Fig. 4). NR analysis revealed that OmpC(Y286A), which has a non-functional internal β-signal in the -5 β-strand, accumulated in that region of the BAM complex corresponding to the POTRA3-4-5 region of BamA and BamD (Fig. 3d, e). The accumulated substrate also had an impact of extending this region of the BAM complex outwards from the membrane by 15 Å (from 30 Å from the membrane interface to 45 Å from the membrane interface) in NR experiments. In terms of the precise residues involved in the BamD-substrate interaction, the crosslinked residues were located on the interior side of the funnel-like structure formed by BamD and POTRA domains (Extended Data Fig. 15). Considering the assembly intermediate of EspP engaged with the BAM complex, the -4 strand begins to interact with the R49 residue of BamD, in the N-terminal substrate binding region, even before the -5 strand had entered into this cavity[12]. Spatially, this means the BamD subunit of the BAM complex can serve to marshal two parts of the nascent OMP substrate within the periplasmic domain of the BAM complex, prior to engagement with the lateral gate of BamA.

We looked in detail at the conformations of the structure of periplasmic regions of the intermediate of the EspP-BAM complex[12]. Considering this in terms of the BAM complex structure is worthwhile, where the N-terminal region of BamD interacts with BamA POTRA1 and POTRA2 (P1-2 hinge), and the C-terminal region interacts with BamA POTRA5 in proximity to the lateral gate (Extended Data Fig. 15)[9,20,21]. The N-terminus of BamD changed conformation depending on the folding states of the last four strands of EspP while the C-terminal section of BamD and POTRA5 stably interacted in this stage of the folding reaction[12]. Thus, the dimensions

of this cavity change depending on the folded state of the substrate engaged in it. Lipidated BamD-conjugated with proteoliposome can assemble substrate BamA into proteoliposome without BamA as machinery[55] and we showed that purified BamD can facilitate partial folding of the C-terminal region of an OMP (Fig. 5b). Collectively, we propose that BamD captures the -1 strand in the C-terminal region and draws the -5 strand by a conformational change in the N-terminal region, thereby stimulating the formation of hydrogen bonds, to form β-hairpins in neighboring strands. This cascade may enhance the efficient folding of the final β-barrel, prior to engagement with the lateral gate of BamA.

The importance of both signal recognition by BamD is clearly demonstrated in the EMM assembly assay (*in vitro* assay) (Fig. 5f) but not *in vivo* (Fig. 6a). Even with two mutations to the signal recognition sites in BamD, *E. coli* remained viable. We observed a reduction in the steady-state level of porin only after extended incubation of the signal recognition site mutants (Fig. 6b, c). Because BamD is the multifunctional organizer of the BAM complex, functioning to organize BamC and BamE against BamA[25,56,57], the essentiality of BamD is not solely dependent on its substrate recognition function[46]. However, the importance of its substrate recognition function is demonstrated in that mutations of the internal β-signal recognition site BamD, as well as overexpression of the internal β-signal mutant substrate, impaired the overall integrity of the OM.

OMPs are the major components of bacterial OMs, accounting for more than 50% of the OM volume[58,59]. The quantitative analysis of single-cell data suggest ~500 of molecules of OmpF need to be assembled into the outer membrane per minute per cell[60,61], meaning that factors that promote the efficiency of OmpF assembly are critical to ensure that *E. coli* can handle this extraordinary rate of substrate protein flux. In order to fight against external insult, all of the Gram-negative bacteria contain BamD, the OMPs assembly accelerator.

References for Main text

1. Klebba, P. E. & Newton, S. M. Mechanisms of solute transport through outer membrane porins: burning down the house. *Current Opinion in Microbiology* **1**, 238–247 (1998).

2. Konovalova, A., Kahne, D. E. & Silhavy, T. J. Outer Membrane Biogenesis. *Annu. Rev. Microbiol*. **71**, 539–556 (2017).

3. Schulz, G. E. β-Barrel membrane proteins. *Current Opinion in Structural Biology* **10**, 443–447 (2000).

4. Heinz, E. & Lithgow, T. A comprehensive analysis of the Omp85/TpsB protein superfamily structural diversity, taxonomic occurrence, and evolution. *Front Microbiol* **5**, 370 (2014).

5. Pfanner, N., Wiedemann, N., Meisinger, C. & Lithgow, T. Assembling the mitochondrial outer membrane. *Nat Struct Mol Biol* **11**, 1044–1048 (2004).

6. Ranava, D., Caumont-Sarcos, A., Albenne, C. & Ieva, R. Bacterial machineries for the assembly of membrane-embedded β-barrel proteins. *FEMS Microbiol Lett* **365**, (2018).

7. Ulrich, T. & Rapaport, D. Biogenesis of beta-barrel proteins in evolutionary context. *Int J Med Microbiol* **305**, 259–264 (2015).

8. Noinaj, N. *et al.* Structural insight into the biogenesis of β-barrel membrane proteins. *Nature* **501**, 385–390 (2013).

9. Tomasek, D. *et al.* Structure of a nascent membrane protein as it folds on the BAM complex. *Nature* **583**, 473–478 (2020).

10. Xiao, L. *et al.* Structures of the β□barrel assembly machine recognizing outer membrane protein substrates. *FASEB j*. **35**, (2021).

11. Takeda, H. *et al.* Mitochondrial sorting and assembly machinery operates by β-barrel switching. *Nature* **590**, 163–169 (2021).

12. Doyle, M. T. *et al.* Cryo-EM structures reveal multiple stages of bacterial outer membrane protein folding. *Cell* **185**, 1143-1156.e13 (2022).

13. Doyle, M. T. & Bernstein, H. D. Bacterial outer membrane proteins assemble via asymmetric interactions with the BamA β-barrel. *Nat Commun* **10**, 3358 (2019).

14. Doyle, M. T. & Bernstein, H. D. BamA forms a translocation channel for polypeptide export across the bacterial outer membrane. *Molecular Cell* **81**, 2000-2012.e3 (2021).

15. Kutik, S. *et al.* Dissecting Membrane Insertion of Mitochondrial β-Barrel Proteins. *Cell* **132**, 1011–1024 (2008).

16. Wang, X., Peterson, J. H. & Bernstein, H. D. Bacterial Outer Membrane Proteins Are Targeted to the Bam Complex by Two Parallel Mechanisms. *mBio* **12**, (2021).

17. Struyvé, M., Moons, M. & Tommassen, J. Carboxy-terminal phenylalanine is essential for the correct assembly of a bacterial outer membrane protein. *J Mol Biol* **218**, 141–148 (1991).

18. Paramasivam, N., Habeck, M. & Linke, D. Is the C-terminal insertional signal in Gram-negative bacterial outer membrane proteins species-specific or not? *BMC Genomics* **13**, 510 (2012).

19. Wu, T. *et al.* Identification of a Multicomponent Complex Required for Outer Membrane Biogenesis in Escherichia coli. *Cell* **121**, 235–245 (2005).

20. Bakelar, J., Buchanan, S. K. & Noinaj, N. The structure of the β-barrel assembly machinery complex. *Science* **351**, 180–186 (2016).

21. Gu, Y. *et al.* Structural basis of outer membrane protein insertion by the BAM complex. *Nature* **531**, 64–69 (2016).

22. Iadanza, M. G. *et al.* Lateral opening in the intact β-barrel assembly machinery captured by cryo-EM. *Nat Commun* **7**, 12865 (2016).

23. Anwari, K. *et al.* The evolution of new lipoprotein subunits of the bacterial outer membrane BAM complex. *Molecular Microbiology* **84**, 832–844 (2012).

24. Webb, C. T., Heinz, E. & Lithgow, T. Evolution of the β-barrel assembly machinery. *Trends Microbiol* **20**, 612–620 (2012).

25. Malinverni, J. C. *et al.* YfiO stabilizes the YaeT complex and is essential for outer membrane protein assembly in *Escherichia coli*: YfiO assembles OMPs and stabilizes the YaeT complex. *Molecular Microbiology* **61**, 151–164 (2006).

26. Voulhoux, R. Role of a Highly Conserved Bacterial Protein in Outer Membrane Protein Assembly. *Science* **299**, 262–265 (2003).

27. Wu, R. *et al.* Plasticity within the barrel domain of BamA mediates a hybrid-barrel mechanism by BAM. *Nat Commun* **12**, 7131 (2021).

28. Imai, Y. *et al.* A new antibiotic selectively kills Gram-negative pathogens. *Nature* **576**, 459–464 (2019).

29. Kaur, H. *et al.* The antibiotic darobactin mimics a β-strand to inhibit outer membrane insertase. *Nature* **593**, 125–129 (2021).

30. Hagan, C. L., Wzorek, J. S. & Kahne, D. Inhibition of the β-barrel assembly machine by a peptide that binds BamD. *Proceedings of the National Academy of Sciences* **112**, 2011–2016 (2015).

31. Celik, N. *et al.* A bioinformatic strategy for the detection, classification and analysis of bacterial autotransporters. *PLoS One* **7**, e43245 (2012).

32. Horne, J. E. & Radford, S. E. Roll out the barrel! Outer membrane tension resolves an unexpected folding intermediate. *Cell* S0092-8674(22)00261–6 (2022) doi:10.1016/j.cell.2022.03.001.

33. Tomasek, D. & Kahne, D. The assembly of β-barrel outer membrane proteins. *Current Opinion in Microbiology* **60**, 16–23 (2021).

34. Gunasinghe, S. D. *et al.* The WD40 Protein BamB Mediates Coupling of BAM Complexes into Assembly Precincts in the Bacterial Outer Membrane. *Cell Reports* **23**, 2782–2794 (2018).

35. Ieva, R., Tian, P., Peterson, J. H. & Bernstein, H. D. Sequential and spatially restricted interactions of assembly factors with an autotransporter domain. *Proceedings of the National Academy of Sciences* **108**, E383–E391 (2011).

36. Leyton, D. L. *et al.* A mortise–tenon joint in the transmembrane domain modulates autotransporter assembly into bacterial outer membranes. *Nature Communications* **5**, (2014).

37. Roman-Hernandez, G., Peterson, J. H. & Bernstein, H. D. Reconstitution of bacterial autotransporter assembly using purified components. *eLife* **3**, (2014).

38. Mannella, C. A., Neuwald, A. F. & Lawrence, C. E. Detection of likely transmembrane beta strand regions in sequences of mitochondrial pore proteins using the Gibbs sampler. *J Bioenerg Biomembr* **28**, 163–169 (1996).

39. Rapoport, T. A. Protein translocation across the eukaryotic endoplasmic reticulum and bacterial plasma membranes. *Nature* **450**, 663–669 (2007).

40. Rocque, W. J. & McGroarty, E. J. Isolation and preliminary characterization of wild-type OmpC porin dimers from Escherichia coli K-12. *Biochemistry* **28**, 3738–3743 (1989).

41. Shen, H.-H. *et al.* Reconstitution of a nanomachine driving the assembly of proteins into bacterial outer membranes. *Nature Communications* **5**, (2014).

42. Ding, Y. *et al.* Characterization of BamA reconstituted into a solid-supported lipid bilayer as a platform for measuring dynamics during substrate protein assembly into the membrane. *Biochimica et Biophysica Acta (BBA) - Biomembranes* **1862**, 183317 (2020).

43. Chen, X. *et al.* Substrate-dependent arrangements of the subunits of the BAM complex determined by neutron reflectometry. *Biochimica et Biophysica Acta (BBA) - Biomembranes* **1863**, 183587 (2021).

44. Burgess, N. K., Dao, T. P., Stanley, A. M. & Fleming, K. G. β-Barrel Proteins That Reside in the Escherichia coli Outer Membrane in Vivo Demonstrate Varied Folding Behavior in Vitro. *Journal of Biological Chemistry* **283**, 26748–26758 (2008).

45. Chin, J. W., Martin, A. B., King, D. S., Wang, L. & Schultz, P. G. Addition of a photocrosslinking amino acid to the genetic code of Escherichia coli. *Proceedings of the National Academy of Sciences* **99**, 11020–11024 (2002).

46. Hart, E. M. & Silhavy, T. J. Functions of the BamBCDE Lipoproteins Revealed by Bypass Mutations in BamA. *J Bacteriol* **202**, e00401-20 (2020).

47. Imai, K., Fujita, N., Gromiha, M. M. & Horton, P. Eukaryote-wide sequence analysis of mitochondrial β-barrel outer membrane proteins. *BMC Genomics* **12**, 79 (2011).

48. Cox, D. L. *et al.* Surface immunolabeling and consensus computational framework to identify candidate rare outer membrane proteins of Treponema pallidum. *Infect Immun* **78**, 5178–5194 (2010).

49. Eddy, S. R. Multiple alignment using hidden Markov models. *Proc Int Conf Intell Syst Mol Biol* **3**, 114–120 (1995).

50. Bailey, T. L. *et al.* MEME SUITE: tools for motif discovery and searching. *Nucleic Acids Research* **37**, W202–W208 (2009).

51. Bitto, E. & McKay, D. B. The periplasmic molecular chaperone protein SurA binds a peptide motif that is characteristic of integral outer membrane proteins. *J Biol Chem* **278**, 49316–49322 (2003).

52. de Cock, H., Struyvé, M., Kleerebezem, M., van der Krift, T. & Tommassen, J. Role of the carboxy-terminal phenylalanine in the biogenesis of outer membrane protein PhoE of Escherichia coli K-12. *J Mol Biol* **269**, 473–478 (1997).

53. Jansen, C., Heutink, M., Tommassen, J. & de Cock, H. The assembly pathway of outer membrane protein PhoE of Escherichia coli. *Eur J Biochem* **267**, 3792–3800 (2000).

54. Robert, V. *et al.* Assembly factor Omp85 recognizes its outer membrane protein substrates by a species-specific C-terminal motif. *PLoS Biol* **4**, e377 (2006).

55. Hagan, C. L., Kim, S. & Kahne, D. Reconstitution of Outer Membrane Protein Assembly from Purified Components. *Science* **328**, 890–892 (2010).

56. Kim, S. *et al.* Structure and Function of an Essential Component of the Outer Membrane Protein Assembly Machine. *Science* **317**, 961–964 (2007).

57. Kim, K. H., Aulakh, S. & Paetzel, M. Crystal Structure of β-Barrel Assembly Machinery BamCD Protein Complex. *Journal of Biological Chemistry* **286**, 39116–39121 (2011).

58. Horne, J. E., Brockwell, D. J. & Radford, S. E. Role of the lipid bilayer in outer membrane protein folding in Gram-negative bacteria. *Journal of Biological Chemistry* **295**, 10340–10367 (2020).

59. Jarosławski, S., Duquesne, K., Sturgis, J. N. & Scheuring, S. High-resolution architecture of the outer membrane of the Gram-negative bacteria Roseobacter denitrificans. *Mol Microbiol* **74**, 1211–1222 (2009).

60. Wiśniewski, J. R. & Rakus, D. Quantitative analysis of the Escherichia coli proteome. *Data Brief* **1**, 7–11 (2014).

61. Benn, G. *et al.* Phase separation in the outer membrane of Escherichia coli. *Proc Natl Acad Sci U S A* **118**, e2112237118 (2021).

ACKNOWLEDGEMENTS

We thank the members of the Shiota, Shen and Lithgow labs for discussion and critical comments on the manuscript. This work was supported by JSPS KAKENHI to T.S. (19K16077, 18KK0197 and 18H06052), to E.M.G. (21K15043), and to K.I. (18K11543 and 21H03551), JST FOREST Program to T.S. (JPMJFR2064), AMED Research Support Project for Life Science and Drug Discovery (Basis for Supporting Innovative Drug Discovery and Life Science Research (BINDS)) (22ama121029j0001) to K.I., Australian Research Council (DP160100227) to T.L, and National Health and Medical Research Council (CDF1106798) to H.-H.S.. The following grants are also acknowledged; a grant from the Ichiro Kanehara Foundation for the Promotion of Medical Sciences and Medical Care, Waksman Foundation of Japan, Tokyo Biochemical Research Foundation, Sumitomo Foundation, Naito Foundation, Uehara Memorial Foundation, The Shinnihon Foundation of Advanced Medical Treatment Research, and Noguchi institute (to T.S.). The NR experiment at the J-PARC MLF was performed under a user program (Proposal No. 2019B0364). We thank N. L. Yamada for support of NR measurements, and H. Nishitoh for access to instruments (for T.S.). Radiation experiment were performed at RI unit of FSRC of UoM.

AUTHOR CONTRIBUTIONS

E.M.G., T.L., and T.S. designed research and wrote the paper. E.M.G. and T.S. performed most of the key experiments. Y.D, E.G. and T.S. measured NR and Y.D., X.F.L and H.-H.S. analyzed NR data. Y.N., K.H., and K.S.T. prepared materials. R.A.D., C.T.W., and C.J.S supervised NR sample preparation. N.T. performed BamD-depletion experiments. K.I performed sequence analysis. R.S.B prepared materials and edited the paper.

MAIN FIGURE LEGENDS

Fig. 1 | BAM complex inhibitor peptides derived from OmpC uncover essential signals in OMP assembly. **a**, ^{35}S-labelled EspP was synthesized by rabbit reticulocyte lysate, then incubated with EMM. At the indicated time, the EMM samples were shifted onto ice to halt assembly reaction, and treated with (+) or without (-) Proteinase K (see Extended Data Fig. 1). Proteins were analyzed by SDS-PAGE and radio-imaging. (p) and (m) indicate to precursor and mature form of EspP, respectively. **b,** EspP assembly into EMM was performed in the presence of DMSO (D) or specific inhibitor peptides. Peptides labelled 1 through 23 were derived from OmpC, while peptide 24 was taken from the yeast mitochondrial β-barrel protein TOM40 to serve as a negative control. Of the peptides, 6 were capable of inhibiting EspP maturation and thus selected to assay against other OMPs. **c**, ^{35}S-labelled OmpA was incubated with EMM then shifted onto ice to halt the assembly reaction at indicated times. Samples were split and incubated at either 25°C or 99°C for 10 min, before analysis by SDS-PAGE and radio-imaging. (p) and (f) indicate precursor or folded, respectively. **d,** Peptide inhibition of assembly reactions for OmpC. ^{35}S-labelled OmpC was incubated as above for indicated time, shifted onto ice, and solubilized in BN-PAGE lysis buffer containing 1.5% DDM. Solutions were clarified via centrifugation and analyzed by BN-PAGE and radio-imaging. The assembled, trimeric form of OmpC is indicated. **e**, Densitometry quantification data of assembled OMPs in the EMM assembly assays. The OMPs include OmpA, OmpC, OmpF, and LamB (n=3). **f,** Sequence comparison of inhibitor peptides isolated from EspP assembly assay. All peptides contain a sequence similar to the β-signal found the in c-terminal β-strand of OMPs. The signal is comprised of key hydrophobic, polar, glycine, and 2 aromatic or hydrophobic amino acids. Amino acids highlighted in blue conform to the signal, while those highlighted in purple deviate. Several peptides assayed contain a similar sequence, however lacked inhibition of OMP assembly. **g,** Peptide 18 was mutated at amino acids of the β-signal. Position 0, the first hydrophobic residue, and position 8, the final aromatic or hydrophobic residue, showed the most sensitivity to mutation, completely losing inhibitory ability.

Fig. 2 | Internal β-signals are necessary for proper OMP Assembly *in vitro* and *in vivo*. **a**, (Top) Representation of OmpC, annotated to show the position of each

β-strand (blue arrows) and the region mimicked in the indicated peptides. (Middle) Sequence logos show the conservation of sequence for the residues in these regions (see Methods), where the height of letter corresponds to the degree of conservation across bacterial species, residues are color-coded: aromatic (orange), hydrophobic (green), basic (blue), acidic (red), polar (sky blue) and proline and glycine (black). (Bottom) EMM assembly assay of OmpC mutants: ^{35}S-labelled OmpC wild-type or mutant proteins were incubated with EMM for 30 or 90 min, and analyzed by BN-PAGE and radio-imaging. **b**, Comparison of amino acids in the final and 5th to final (-5) β-strands of OmpC, OmpF, and LamB. All three OMPs contain the putative hydrophobic residue near the N-terminal region of the β-strands, highlight with a black box. A hydrophobic and an aromatic residue is also found to be highly conserved between these OMP β-strands at the C-terminal amino acids of the β-strands. **c**, EMM assembly assay of OmpF mutated at residues in the 5th to last (-5) and 3rd to last (-3)β-strand. Mutations to either β-strand show impaired assembly compared to WT. **d**, Schematic model of FLAG-OmpC expression system in *E. coli*. The plasmid-borne copy of OmpC was mutated and the mutant proteins are selectively detected with antibodies to the FLAG epitope. **e**, Total cell lysates were prepared from the variant *E. coli* strains expressing FLAG-OmpC (WT), -5 strand mutants: F280A, Y286A, double mutant F280A/Y286A (FY), or final β-strand mutants: V359A, Y365A, double mutant V359A/Y365A (VY) with (+) or without (-) arabinose. The steady-state levels of the indicated proteins were assessed after SDS-PAGE by immunoblotting with anti-FLAG antibody. **f**, After growth with arabinose induction, EMM fraction was isolated from each of the FLAG-OmpC variant expressing *E. coli* strains to assess steady state levels of OmpC variants and BAM Complex proteins: BamA, BamB, BamC, BamD, and BamE by SDS-PAGE and immunoblotting. **g**, EMMs, isolated as in (**f**), were solubilized with 1.5% DDM and subjected to BN-PAGE and immunoblotting. The indicated proteins were detected by anti-FLAG (top) and anti-BamA antibodies (bottom), respectively. Double mutations to either the -5 or final β-strand resulted in assembly defects of FLAG-OmpC, while BAM complex remained intact.

Fig. 3 | Analysis of internal β-signal mutant high molecular weight intermediate species. a, (top) Assembly assay of ^{35}S-OmpC and -5 internal β-signal mutant Y286A. Radio-labelled protein was incubated with EMM for indicated time points, then

resolved via BN-PAGE. OmpC trimer and intermediate are indicated. (bottom) Quantification of intermediate compared to total assembled protein of 3 independent experiments. **b**, BN-PAGE analysis of ^{35}S-labelled OmpC(Y286A) incubated with EMM for 60 mins. The EMM fraction was solubilized with 1.5% DDM and incubated with (+) or without (-) anti-BamC antibody for 40 min and the samples analyzed by BN-PAGE. The presumptive translocation intermediate (Int) and the gel-shift species (Int+AB) are indicated. **c**, ^{35}S-labelled OmpC was incubated with EMM and then analyzed by BN-PAGE and radio-imaging. EMM were then washed and solubilized in the presence (+) or absence (-) of 6 M urea, after which the membrane fraction was re-isolated via ultra-speed centrifugation for 45 min. Isolated membranes were solubilized in 1.5% DDM and analyzed by BN-PAGE. **d**, NR profiles for BamA in membrane (1st measurement, square black line), BamA-D (2nd measurement, circle red line), and BamAD-substrate (3rd measurement, triangle blue line). **e**, Table summarizes of the thickness, volume fraction, and roughness of NR analysis. 1st, 2nd, and 3rd measurement displayed in black, magenta, and blue, respectively. P3-5: POTRA3, POTRA 4, and POTRA5, P1-2: POTRA1 and POTRA2, Lipid: POPC, Solution: D_2O, gold match water (GMW) and H_2O. Details were described in Table S8 to S10. **f**, Neutron reflectometry schematic of BamA-D complex dynamics with internal β-signal mutant OmpC. Green, yellow, and magenta indicate BamA, BamD and OmpC(Y286A), respectively. Numbers indicate corresponding POTRA domains. **g**, Urea-denatured OmpC variants were folded into DDM-micelles in 10 mM phosphate buffer (pH 8.0), 2 mM EDTA, and 1 mM glycine. Samples were incubated at 37°C for up to 36 hours then split with half boiled. OmpC showed two clear species, a trimeric assembled and monomeric unfolded.

Fig. 4 | BamD acts as the receptor for internal β-signals. a, Ni-NTA was used to affinity purify His6-BamA or His6-BamD. The BAM complex protein-Ni-NTA bead complex were then incubated in the presence of DMSO or inhibitor peptide which contained either internal β-signals, 18 and 21, or canonical final β-signal, 23. Finally ^{35}S-labelled OmpC was added to the beads. Beads were then washed with 20 mM imidazole containing buffer A and proteins were eluted with 400 mM imidazole buffer. BamD pull-down of OmpC was greatly inhibited by both internal β-signal peptides, while BamA was primarily inhibited by the canonical β-signal peptide. The graph represents densitometry analysis of data from 3 independent experiments. **b**, BamD-cys mutant

proteins were purified and incubated with ^{35}S-OmpC with cysteine mutations from the -5 to the final β-strand. After the addition of the oxidizing agent, $CuSO_4$, samples were purified with Ni-NTA and analyzed by SDS-PAGE. BamD carrying cys mutations in the N-terminus formed disulfide bonds in near regions containing internal β-strands, with C-terminal BamD-cys forming disulfide bonds primarily in the final β-strand. **c**, BamD cysteine mutants, highlighted in magenta, formed disulfide bonds at distinct locals of OmpC. **d**, BPA containing BamD was expressed in the presence (+) or absence (-) of FLAG-OmpC overexpression. Pink arrows indicate BamD-FLAG-OmpC cross-link products.

Fig. 5 | Residues in the N- and C- terminal of BamD marshal OMPs for proper assembly. a, Double cysteine residues were mutated into OmpC between anti-parallel β-strands to form artificial disulfide bonds (Left). ^{35}S-OmpC-cys variants were translated then incubated with (+) or without (-) BamD. The samples were analyzed by reducing or non-reducing condition. Disulfid bond formed bands were indicated the right of the gel. **b**, Sequence conservation analysis of BamD. Target residues, Y62 and R197, are indicated with dark pink spheres on the crystal structure of BamD, sequence logos represent conservation in the immediate region of these residues. Amino acids listed above logo sequence are from crystal structure. **c**, Schematic depiction of the BamD depletion strain of *E. coli* used to express mutant BamD proteins. **d**, Pull-down assay of the variants of BamD-His8. The EMMs as in (**c)** were solubilized with 1.5% DDM and then subjected to Ni-NTA. T- 5% total input, F- unbound fraction, W- wash fraction, E- Eluted fraction. Each fraction was analyzed by SDS-PAGE and immunoblotting against indicated antibodies. **e**, Assembly of OmpC was reduced in EMMs containing BamD mutated at Y62 and R197. ^{35}S-labelled OmpC was incubated with EMM as in (**c**), and then analyzed by BN-PAGE and radio-imaging.

Fig. 6 | BamD substrate recognition is essential to maintain membrane integrity in cells. a, BamD depletion strains were able to grow in restrictive media (LB supplemented with 0.5% glucose) until cells were split and restarted. Mutations to substrate recognition site of BamD were able to grow similar to WT BamD. **b**, Steady state levels of BamD mutant strains in EMM. Protein levels of BAM complex proteins, and OmpF were stable between WT, Y62A, R197A mutants. Wedge indicates that in each case, two samples

were assessed corresponding to either 4 μg or 12 μg of total EMM protein. **c**, OmpF complex formation in BamD mutant expressing cells. BAM complex was used for protein loading control. **d-g,** Growth of cells in the presence of the antibiotic vancomycin (VCN). BamD depletion cells and BamD Y62A mutants were unable to grow in the presence of VCN (**e**). *E coli* cells expressing mutations at two key residues in the -5 internal β-signal of OmpC were sensitive to the presence of VCN. **h**, Structure of BamD (top) and the final 5 β-strands of OmpC (bottom). Gray boxes indicate relative regions of interaction between BamD and substrates. **i**, OmpF complex assembly *in vivo* of cells expressing mutant OmpC. OmpF assembly was greatly reduced in cells expressing double mutations to the -5 internal β-signal.

Fig. 7 | Internal β-signals are conserved in mitochondrial OMPs are remain essential for protein assembly. a, Comparison of the yeast scTom40 protein final β-strand and the -5 strand. Residues of the β-signal are highlighted by gray bars and black boxes. **b,** Web Logo of Tom40 -5 β-strand. Color scheme is as listed above. Amino acids of the β-signal are marked by arrow heads below. **c,** ^{35}S-labeled Tom40 were imported into isolated yeast mitochondria for times indicated. Two intermediate species are found during Tom40 import, intermediate I (Int. I) consists of Tom40-SAM complex and intermediate II (Int. II) Tom40 and Tom5. Mutations to both the final β-strand (L357A and F359A) and the -5 β-strand (Y307A, Y309A, and triple mutant) result in loss of full TOM complex assembly. **d,** Pulse-chase of Tom40 internal β-signal mutants. Mitochondria were incubated with ^{35}S-Tom40 for 5 minutes then harvested. Mitochondria were washed to remove non-imported Tom40 and resuspended in import buffer before allowing the reaction to continue. Samples were collected at indicated time points.

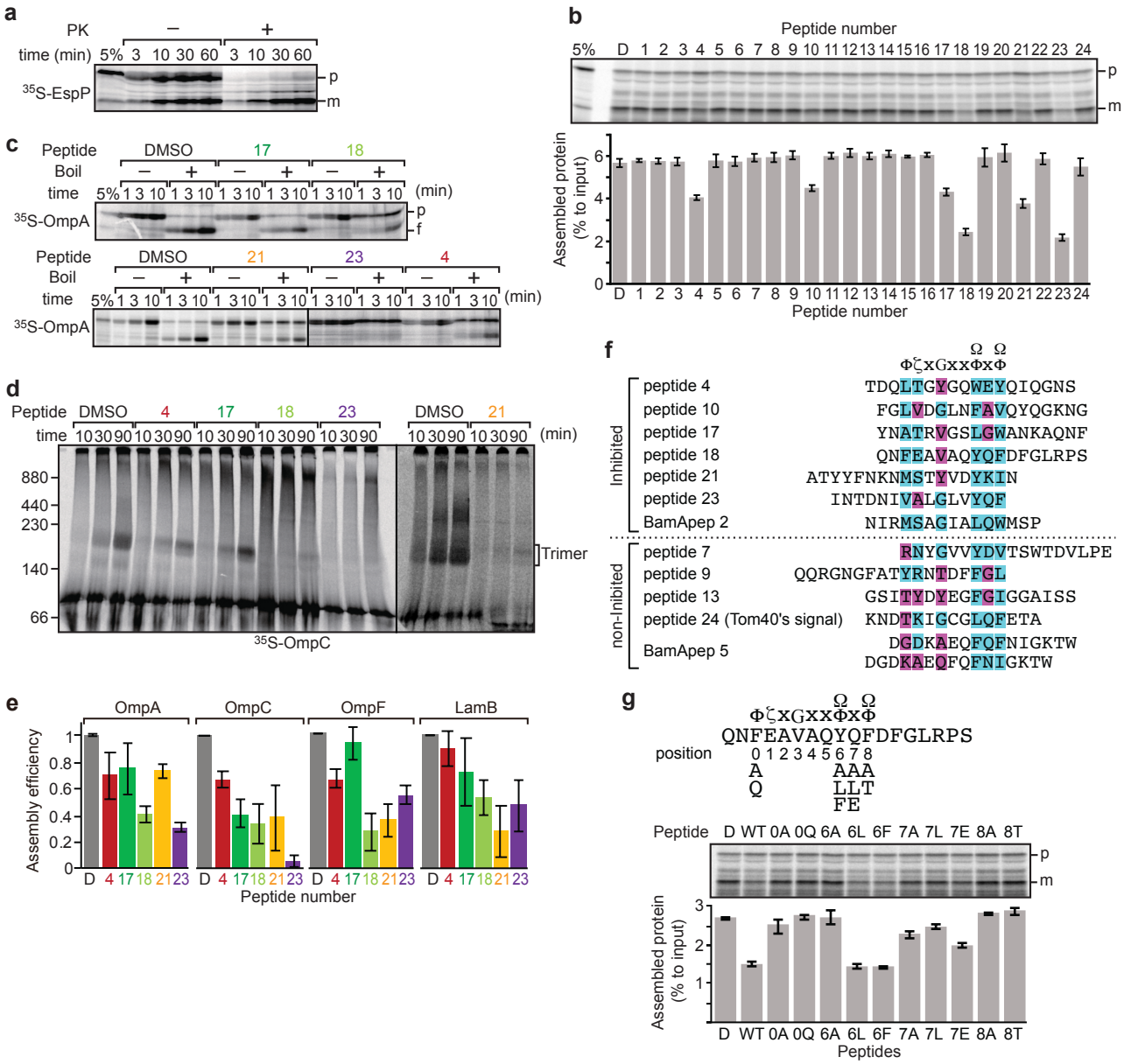

Germany et al. Fig. 1

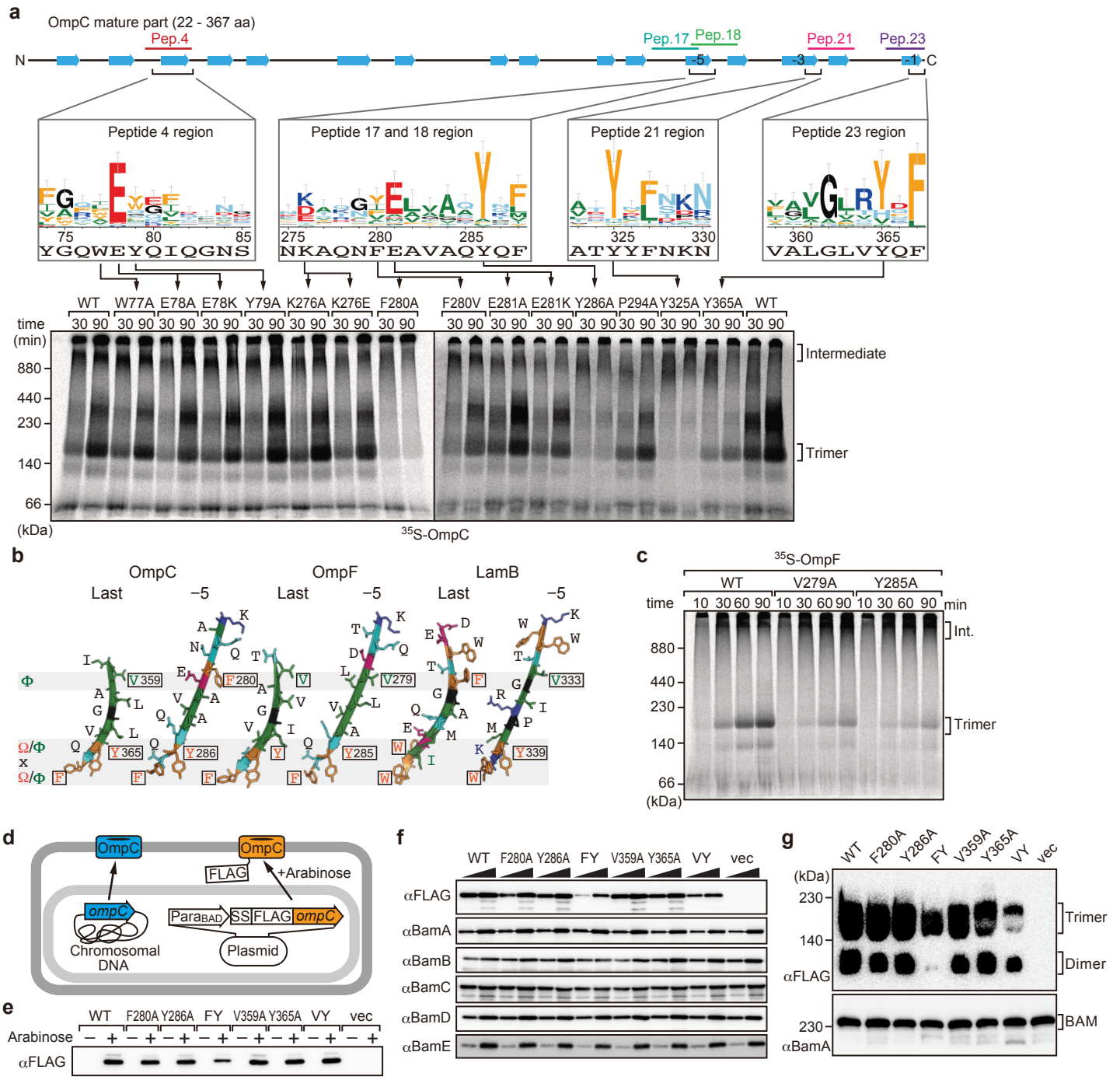

Germany et al. Fig. 2

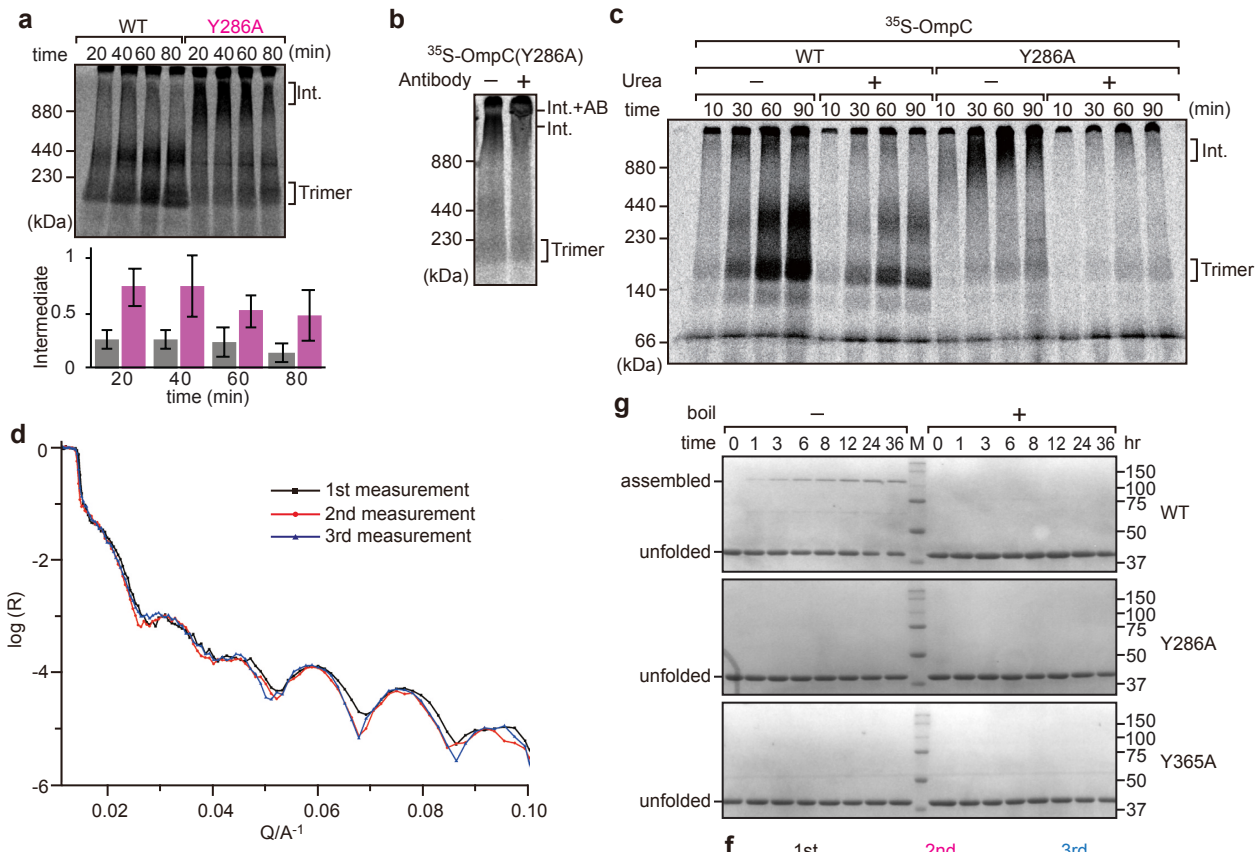

e

	1st measurement	2nd measurement	3rd measurement			
Layers	Thickness (Å)			Roughness (Å)		
His_8	6.0±0.5	7.1±0.8	9.4±0.5	4.0±0.1	4.0±0.1	4.0±0.1
β-Barrel	56.9±1.5	58.7±0.4	56.8±1.5	10.1±0.1	12.6±1.8	6.0±0.1
P3-5	29.5±0.8	29.7±0.8	45.5±1.6	7.0±0.1	6.1±0.1	12.1±0.1
P1-2	31.2±0.8	30.3±0.4	28.5±0.9	13.8±0.1	13.7±0.1	5.0±0.1

f

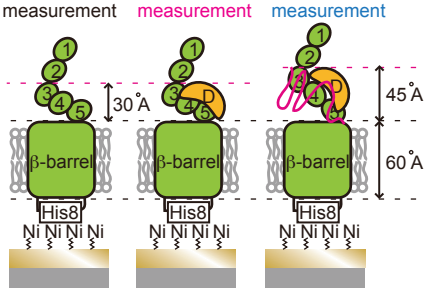

	Volume fraction (%)											
	BamA			POPC			BamD		OmpC	Solution		
His_8	---	---	---	---	---	---	---	---	---	25.3±7.4	25.8±7.0	22.7±1.7
β-Barrel	17.1±0.6	18.4±1.1	18.3±1.2	35.1±1.6	35.4±5.5	35.9±1.5	---	---	---	47.6±2.9	46.2±6.7	45.8±2.7
P3-5	10.7±0.9	11.0±0.8	11.7±2.9	3.4±1.7	3.3±0.5	3.3±0.9	8.8±1.1	9.0±3.3	8.0±1.2	85.9±2.6	76.9±2.0	76.0±7.3
P1-2	11.2±0.8	11.2±2.9	10.7±0.9	---	---	---	---	---	---	90.0±2.5	88.8±2.9	89.3±0.9

Germany et al. Fig. 3

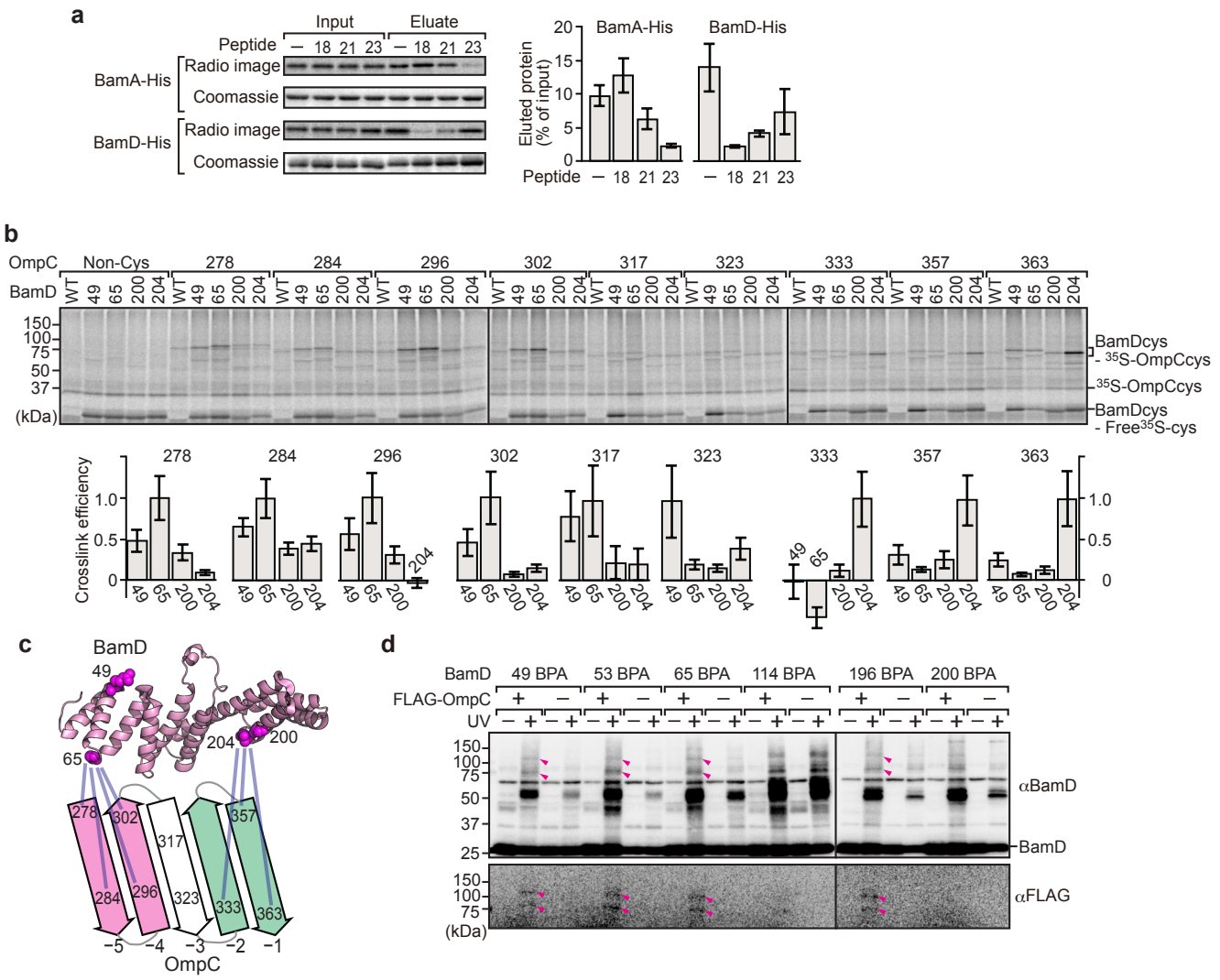

Germany et al. Fig. 4

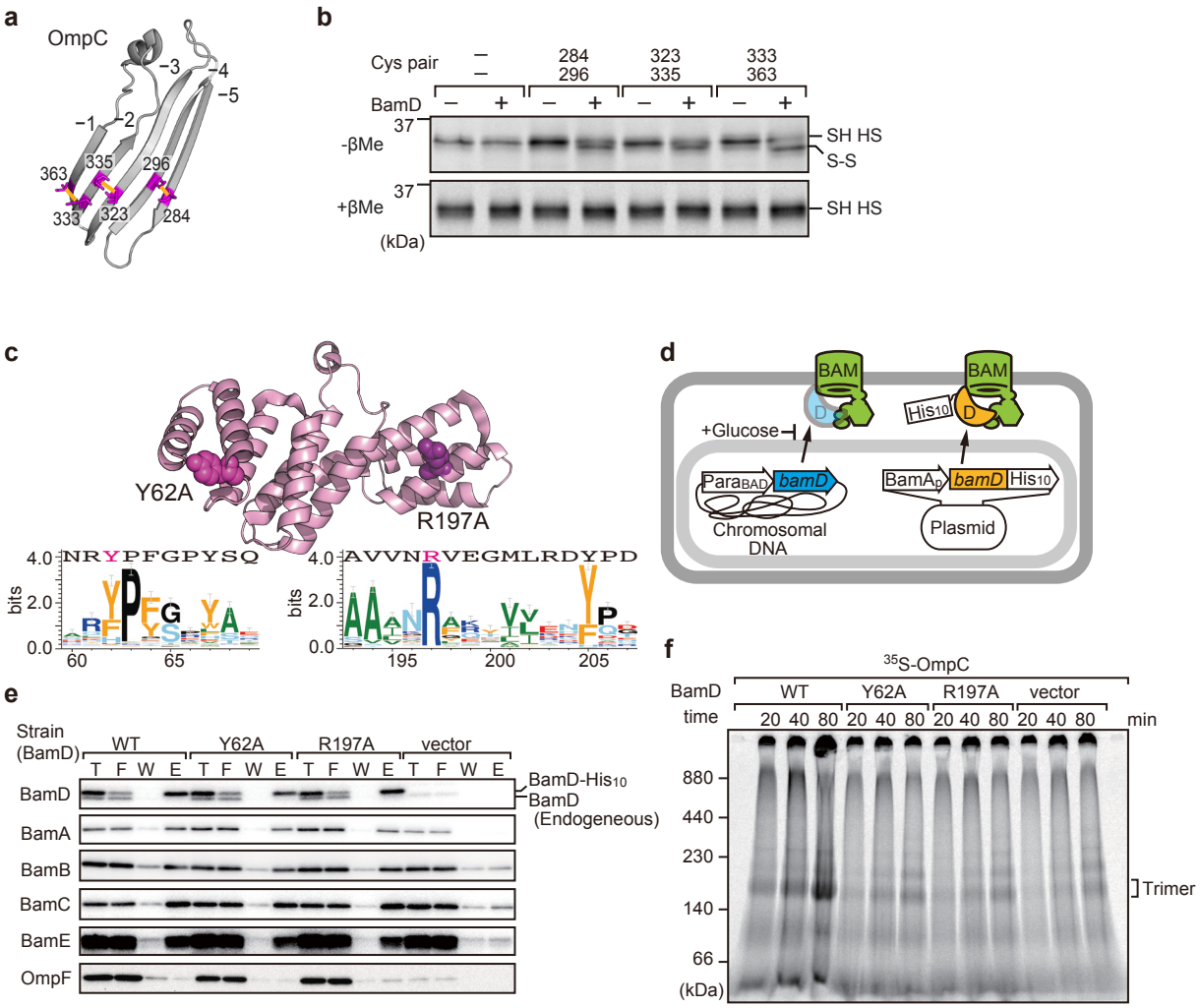

Germany et al. Fig. 5

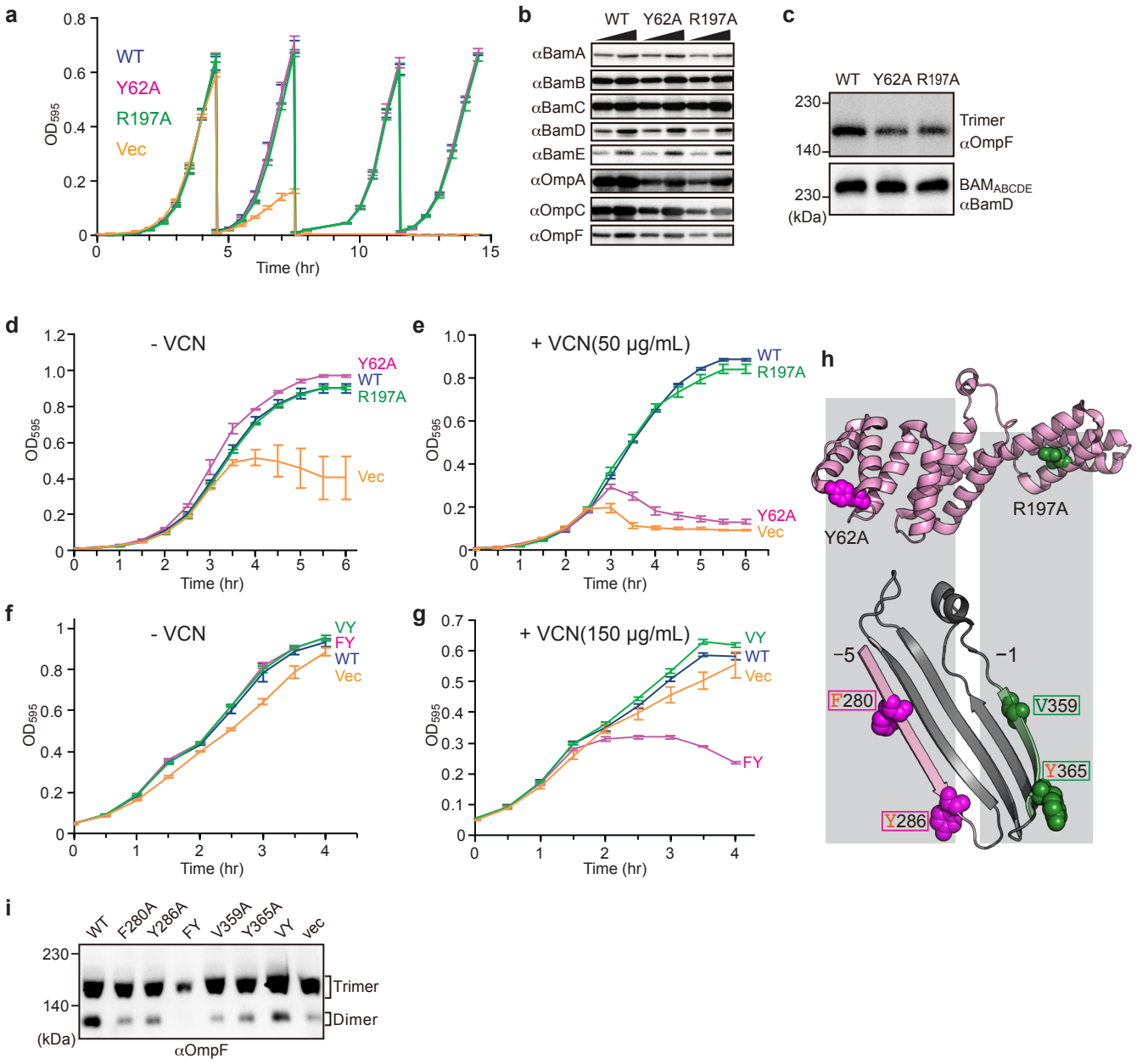

Germany et al. Fig. 6

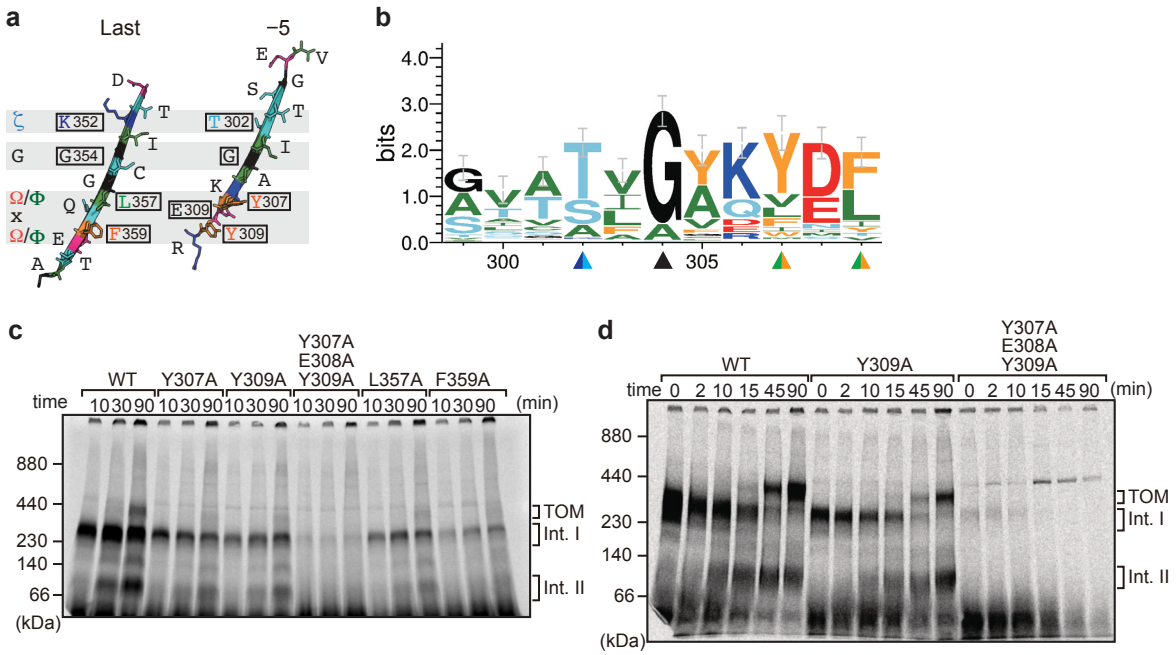

Germany et al. Fig. 7